LUND UNIVERSITY

Lung mechanics in the aging lung and in acute lung injury. Studies based on sinusoidal flow modulation.

Bitzén, Ulrika

2006

Lund University, Faculty of Medicine Doctoral Dissertation Series 2006:83

Lung mechanics in the aging lung and in acute lung injury

Studies based on sinusoidal flow modulation

ULRIKA BITZÉN, M.D.

LUND UNIVERSITY

Doctoral Thesis
2006

Department of Clinical Physiology
Lund University, Sweden

Faculty opponent
Professor Göran Hedenstierna, Department of Clinical Physiology, Uppsala University, Sweden

The public defense of this thesis will, with due permission from the Faculty of Medicine at Lund University, take place in Föreläsningssal 1, Lund University Hospital, on Wednesday, June 14, 2006, at 1.00 pm.

ISSN 1652-8220
ISBN 91-85559-07-5

ulrika.bitzen@med.lu.se

Department of Clinical Physiology, Lund University
SE-221 85 LUND, Sweden

A full text electronic version of this thesis is available at
http://theses.lub.lu.se/postgrad

Typeset using LaTeX and the template lumedthesis.cls ver 1.0,
available at http://www.hedstrom.name/lumedthesis

Printed by: KFS AB, Lund, Sweden

Contents

List of Papers

This thesis is based on the following papers, which in the text will be referred to by their Roman numerals.

I. Bitzén U, Drefeldt B, Niklason L, Jonson B. Dynamic elastic pressure-volume loops in healthy pigs recorded with inspiratory and expiratory sinusoidal flow modulation. Relationship to static pressure-volume loops. *Intensive Care Med* 2004;30(3):481–488.

II. Bitzén U, Enoksson J, Uttman L, Niklason L, Johansson L, Jonson B. Multiple pressure-volume loops recorded with sinusoidal low flow in a porcine acute respiratory distress syndrome model. *Clin Physiol Funct Imaging* 2006;26(2):113–119.

III. Bitzén U, Niklason L, Drefeldt B, Göransson I, Jonson B. Sinusoidal flow modulation for studies of bronchial and lung parenchyma mechanics. *Manuscript*

IV. Bitzén U, Göransson I, Niklason L, Jonson B. Age dependence of elastic and resistive properties of the lung in a reference population. *Manuscript*

Summary

Knowledge about lung mechanics is of interest in intensive care to adjust mechanical ventilation and in the lung laboratory for diagnostics and evaluation of patients with various kinds of respiratory diseases.

In mechanical ventilation a single inspiratory elastic pressure-volume (P_{el}/V) curve is difficult to interpret due to continuing re-expansion of collapsed lung units over a large pressure interval. However, the volume shifts between multiple inspiratory P_{el}/V curves recorded at different levels of positive end-expiratory pressure (PEEP) give information about lung collapse and re-expansion. Methods based on flow interruption for measurement of P_{el}/V curves have limitations due to continuing gas exchange, the need for disconnection from the ventilator or the fact that they are time consuming. Recordings during constant or sinusoidal flow can be obtained using a computer-controlled ventilator. Sinusoidal flow modulation provides the possibility to separate the elastic and resistive pressure components of measured pressure, thereby providing more accurate inspiratory P_{el}/V curves and simultaneous data of resistance (R) in short time.

The sinusoidal flow modulation method was further developed to allow recording and analysis of both inspiratory and expiratory limbs of P_{el}/V loops and to allow automatic recording of P_{el}/V loops from multiple PEEP levels. P_{el}/V loops obtained by the sinusoidal flow modulation method and by the flow-interruption method were compared in healthy pigs and in pigs with acute lung injury/acute respiratory distress syndrome (ALI/ARDS). Viscoelastic phenomena caused differences in P_{el}/V loops and influenced hysteresis. Lung collapse and re-expansion at decreasing PEEP levels could, however, be estimated by hysteresis of the P_{el}/V loops recorded from zero end-expiratory pressure as well as by the volume shifts between multiple inspiratory P_{el}/V curves recorded at different levels of PEEP. In ALI/ARDS pigs, expiratory R increased during expiration warranting determination of its volume dependence to obtain as accurate dynamic expiratory P_{el}/V curves as possible.

In the lung laboratory lung parenchyma properties and intrinsic bronchial properties are uniquely reflected in the P_{el}/V and elastic pressure-resistance (P_{el}/R) diagrams, respectively, measured at regulated flow rate. The flow-regulation method, previously based on square wave flow modulation ($\dot{V}$square method), was further developed applying sinusoidal flow rate adapted to body size ($\dot{V}$sine method) and iterative parameter estimation for mathematical characterization of P_{el}/V, P_{el}/C and P_{el}/R curves. The quality of results obtained with the $\dot{V}$sine method was equal to that of the more time consuming $\dot{V}$square method. In healthy subjects no effect of heart artefact correction was found. For the $\dot{V}$sine method representative reference values, based on 60 healthy 20–65 year old never-smokers, are presented for P_{el}/V, P_{el}/C and P_{el}/R curves. After normalization to lung size women and men had similar lung mechanics. By relating the P_{el}/V, P_{el}/C and P_{el}/R curves to age and lung size normal ranges were importantly narrowed. Elastic recoil pressure (P_{el}) decreased with age to an extent in agreement with the higher rates observed in previous studies. The width of the normal range for the P_{el}/V curve increased with age indicating individual rate of aging as in the skin. At P_{el} 5 cmH_2O, roughly corresponding to functional residual capacity, compliance (C) increased with age as previously observed. At P_{el} values $\geq$10 cmH_2O C decreased with age. The findings may suggest that the lower part of the P_{el}/V curve in old subjects is influenced by collapsing alveoli, while in younger subjects airway closure dominates. Expiratory R in relation to P_{el} decreased with age. When C and R were related to volume rather than to P_{el} no age dependence was observed. Accordingly, dimension of the lung rather than the distending pressure P_{el} seems to be a determinant of C and R.

Populärvetenskaplig sammanfattning

Avhandlingen har fokus på lungornas mekaniska egenskaper hos friska och vid akut lungskada och på metodutveckling för studier av lungmekanik. Kunskap om lungmekanik är av intresse inom intensivvården för att skräddarsy respiratorbehandling och i lunglaboratoriet för diagnostik och utvärdering av patienter med olika typer av lungsjukdom.

Vid respiratorbehandling kan föreliggande lungskada förvärras om lungdelar under varje andetag kollaberar och re-expanderas. En kurva som avspeglar lungans elastiska återfjädringstryck mot lungvolym kallas P_{el}/V-kurva. Jämfört med en enstaka inspiratorisk P_{el}/V-kurva ger multipla P_{el}/V-kurvor registrerade från olika trycknivåer säkrare information om sådan kollaps och re-expansion.

I delarbete 1 visades hos friska grisar att dynamiska P_{el}/V-kurvor registrerade under flöde ger väsentligen samma information som mer tidskrävande registrering av statiska kurvor, som mäts efter avbrott i flödet.

I delarbete 2 automatiserades metoden för registrering av multipla dynamiska P_{el}/V-kurvor. Hos grisar med akut lungskada visades att sådana kurvor, liksom studier av P_{el}/V-kurvors skillnad mellan in- och utanding (hysteres), ger god upplysning om lungornas kollapsbenägenhet.

I delarbete 3 presenteras en vidareutveckling och validering av flödesregulatormetoden använd inom klinisk fysiologisk diagnostik. Principer som hämtades från delarbete 1 och 2, omfattar sinusoidal flödesmodulering med matematisk analys och matematisk karakterisering av kurvor som beskriver lungvolym, tänjbarhet och flödesmotstånd i förhållande till lungans elastiska återfjädringstryck. Med den nya metoden erhålles motsvarande information med bibehållen kvalitet från betydligt färre andningsmanövrer jämfört med den tidigare använda flödesregulatormetoden baserad på ”fyrkant-modulering” av flödet. Den matematiska karakteriseringen av nämnda kurvor underlättar datalagring och forskning.

I delarbete 4 tillämpas ovanstående metod för studier av friska män och kvinnor, 20–65 år gamla. Mera detaljerat än i tidigare studier visas hur normalt

åldrande påverkar lungornas mekaniska egenskaper. Studien ger också normalvärden för personer av given ålder och kroppsstorlek att använda i klinisk diagnostik.

Abbreviations

ALI	acute lung injury
ARDS	acute respiratory distress syndrome
C	compliance
$C_{5\text{-}15}$	compliance measured over the P_{el} interval 5 to 15 cmH_2O
ECG	electrocardiogram
F_IO_2	fraction of oxygen in inspired air
FRC	functional residual capacity
LIP	lower inflection point
P_{ao}	pressure at airway opening
P_aO_2	partial pressure of oxygen in arterial blood
PEEP	positive end-expiratory pressure
P_{el}	elastic recoil pressure
$P_{el,TLC}$	elastic recoil pressure at total lung capacity
P_L	transpulmonary pressure
P_{LIP}	pressure at the lower inflection point
P_{oe}	oesophageal pressure
P_{res}	resistive pressure
P_{tr}	tracheal pressure
R	resistance
RV	residual volume
TGV	thoracic gas volume
TLC	total lung capacity
TLC_P	predicted total lung capacity
UIP	upper inflection point
V	volume
VC	vital capacity

ΔV_{DER}	de-recruitment volume; volume difference between the beginning of an inspiratory dynamic P_{el}/V curve recorded from PEEP and the inspiratory dynamic P_{el}/V curve recorded from ZEEP
ΔV_{hyst}	volume difference between the inspiratory and expiratory limb of a P_{el}/V loop
$\dot{V}$	flow rate
$\dot{V}_{ao}$	airflow rate
$\dot{V}_{box}$	box flow rate
$\dot{V}$sine method	sinusoidal flow modulation method
$\dot{V}sine_{corr}$ method	$\dot{V}$sine method with heart artefact correction
$\dot{V}sine_{uncorr}$ method	$\dot{V}$sine method without heart artefact correction
$\dot{V}$square method	square wave flow modulation method
ZEEP	zero end-expiratory pressure

All flow and volume data refer to BTPS conditions

Chapter 1

Introduction

1.1 Information provided by lung mechanics

Studies of lung mechanics provide important information beyond the information obtained from spirometry.[1] As a complement to spirometry, such information can be crucial for correct diagnosis in lung disease. Properties of the lung parenchyma and bronchi are uniquely reflected in the elastic pressure-volume (P_{el}/V) and elastic pressure-resistance (P_{el}/R) diagrams, respectively. Among patients with chronic obstructive pulmonary disease (COPD) emphysema and intrinsic bronchial obstruction contribute to obstruction in highly varying degree. Lung mechanics allow differentiation between these components of obstruction.[2] Another example is the value of measuring resistance in the selection of patients with COPD suitable for lung volume reduction surgery.[3] Restriction due to increased stiffness of the lungs can be separated from conditions with restriction due to neuromuscular or thoracic cage disease.[4] Studies of P_{el}/V and P_{el}/R relationships have contributed to the knowledge about different restrictive lung diseases.[5–8]

1.2 Effects of aging on lung mechanics

Several early studies have shown that the elastic recoil pressure of the lung (P_{el}) at a certain lung volume (V) decreases with increasing age.[9–13] The limited information available about age dependence of compliance (C) refers to the volume range around the tidal volume.[10, 13–16] Age dependence of expiratory lung resistance (R) appears not to have been studied. Other limitations are that previous studies were not based on a random selection from the population, included smokers or were based on small materials.

No previous study of aging integrates the wider aspect comprised in P_{el}/V, elastic pressure-compliance (P_{el}/C) and P_{el}/R curves. In our department a non-published reference material that is not based on a random selection from the population, has been used.

1.3 Acute lung injury/Acute respiratory distress syndrome

The acute respiratory distress syndrome in adults (ARDS) and principles for mechanical ventilation were first outlined by Ashbaugh et al.[17] Acute lung injury (ALI) and/or ARDS may follow, for example, from infection, trauma, aspiration, chemical pneumonitis and pancreatitis. ALI and ARDS represent different severities of lung injury, ARDS being the more severe form. The early phase of ALI/ARDS is characterized by epithelial damage, inflammation, oedema and hyaline membranes in peripheral lung. A physiological consequence is an increased tendency for lung collapse leading to atelectasis formation with shunting of venous blood through the lung resulting in hypoxemia. Decreased diffusing capacity due to oedema and hyaline membranes contribute to the hypoxemia.

In mechanical ventilation ALI/ARDS can be worsened or even induced by ventilation patterns resulting in cyclic lung collapse and re-expansion and/or over-distension. To avoid traumatic ventilation of the lungs, ventilator setting should be adapted to the actual status of the individual patient. The inspiratory P_{el}/V curve recorded from zero end expiratory pressure (ZEEP) may be used as guideline for ventilator setting in acute lung injury.[18,19] However, several studies illustrate difficulties in interpreting a single P_{el}/V curve.[20–23] Multiple inspiratory P_{el}/V curves recorded from different levels of positive end-expiratory pressure (PEEP) and from ZEEP provide more detailed information about pressures at which lung collapse and re-expansion occur.[24–26] An alternative is to record P_{el}/V loops comprising inspiratory and expiratory P_{el}/V curves.[27–29]

1.4 Methods for determination of P_{el}/V and P_{el}/R diagrams

Recordings of lung mechanics are based on measurements of transpulmonary pressure (P_L) or pressure in the airway (P_{tr}). P_L and P_{tr} comprise both elastic pressure (P_{el}) and resistive pressure (P_{res}) (P_L or $P_{tr} = P_{el} + P_{res}$) that need to be separated.

In the absence of flow, P_L or P_{tr} equals P_{el}. Methods to determine P_{el} have therefore often been based on measurements during flow interruption. In the lung laboratory P_L is measured as the pressure difference between mouth piece and oesophagus, the latter pressure representing pleural pressure. In mechanical ventilation P_{tr} may be estimated from ventilator pressure minus resistive pressure drop in the connecting tubes.

P_{res} depends on flow rate ($\dot{V}$) and resistance (R):

$$P_{res} = R \times \dot{V} \Longleftrightarrow R = P_{res}/\dot{V} \tag{1.1}$$

At turbulent flow R increases with flow rate according to Rohrer :[30]

$$R = K_1 + K_2 \times \dot{V} \Longleftrightarrow P_{res} = K_1 \times \dot{V} + K_2 \times \dot{V}^2 \tag{1.2}$$

The radius of the airway depends on intrinsic airway properties and the distending pressure P_{el}. Thereby airway resistance varies with P_{el}. In order to determine the intrinsic properties of the bronchi, it is important that R is measured at a standardized flow rate and related to P_{el}.

P_{el}/V recording in the lung laboratory

The idea to regulate flow rate during an intermittently interrupted expiration was introduced by Allander et al.[31] The flow-regulator method, further developed by Jonson,[32] is based on regulation of expiratory flow into small square waves. It has been further refined by combining the measurements with body plethysmography for determination of absolute thoracic gas volume (TGV).

A limitation of the flow-regulator method is that for each square flow wave only a single point is obtained in a P_{el}/V or P_{el}/R diagram. Furthermore, the information is affected by noise in P_L. Noise is caused by sudden accelerations and decelerations of flow associated with the square wave flow pattern and by heart artefacts. To assure valid information despite this noise, recordings during several deep expirations are performed. With this method P_{el}/V and P_{el}/R curves have not been mathematically characterized, but were manually derived from measured points.

P_{el}/V recording in mechanical ventilation

P_{el}/V recordings can be based on either static or dynamic measurements. For static P_{el}/V curves flow dependent P_{res} and volume dependent P_{el} are separated by stopping flow at different volume intervals. The super-syringe method[33] and the flow-interruption method[34] allow determination of static P_{el}/V loops. These

methods have important limitations. Recording with the super-syringe method requires disconnection from the ventilator, and errors may be induced due to continuing gas exchange, particularly during recording of the expiratory limb of a P_{el}/V loop.[35,36] The flow-interruption method is time consuming since only one measurement point in a P_{el}/V diagram is obtained for each interrupted breath. With the slow inflation or pulse method, recordings are performed at very low flow rates minimizing the influence of P_{res}.[37]

A complete P_{el}/V curve can be recorded in a few seconds by allowing a higher flow rate. Then, P_{res} needs to be subtracted on the basis of a known value of R. By subtraction of P_{res}, based on R measured over an ordinary preceding breath, dynamic P_{el}/V curves equivalent to static P_{el}/V curves were obtained in a few seconds.[38] During P_{el}/V recording R may differ from R measured under other conditions leading to errors in the P_{el}/V curve. Variations in R occurring during an expiration will lead to such errors.

By using sinusoidal flow modulation rather than constant flow, R can be simultaneously determined with the P_{el}/V curve during a single inspiration.[24,39] Separation of P_{el} and P_{res} was achieved by mathematical modelling of the P_{el}/V curve and iterative analysis based on an equation summing P_{el} and P_{res}. When R is not constant, the variation of R during the measurement also needs to be modelled.

The sinusoidal flow modulation method was not previously developed for recordings of expiratory dynamic P_{el}/V curves. Accordingly, P_{el}/V loops have not been studied with this technique. P_{el}/V loop recordings have been based on the super-syringe method, the flow-interruption method or constant flow, all of which have limitations as discussed above.

1.5 Viscoelastic influence of dynamic P_{el}/V recordings

P_{el}/V recordings performed during continuous flow are often denoted 'dynamic'. To be clinically useful in intensive care, recording and analysis must be fast and convenient, which requires dynamic recording.

In contrast to truly static recordings, dynamic recordings are influenced by viscoelastic phenomena. During the initial part of dynamic lung inflation or expiration at constant flow a viscoelastic pressure builds up until it reaches a steady state level.[40,41] Viscoelastic pressure contributes to hysteresis in dynamic P_{el}/V loops. In rabbits, at the end of insufflation at high degree of lung distension, Svantesson et al. found that the steady state level of viscoelastic pressure was interrupted and that viscoelastic pressure increased further.[42]

Some information is available about differences between static and dynamic P_{el}/V curves, but it is limited to inspiratory curves.[38,43]

1.6 Hysteresis

Hysteresis in P_{el}/V loops can, in principle, reflect surface tension hysteresis, lung collapse/re-expansion and viscoelastic phenomena. The influence of surface tension hysteresis to P_{el}/V hysteresis is debated. Early observations in healthy humans by Mead et al. showed trivial hysteresis for breaths starting from normal functional residual capacity (FRC).[44] Furthermore, in anaesthetized humans, hysteresis was non-significant for normal tidal volumes.[45] Svantesson et al. developed the technique for static P_{el}/V recording to avoid foreseeable errors, but could still not identify static hysteresis in healthy rabbits.[42]

1.7 Mathematical modelling of P_{el}/V curves

Mathematical characterization facilitates handling of data. In 1964 Salazar and Knowles presented the original three-parameter mathematical P_{el}/V model.[46] Increasing degrees of freedom can be achieved by a higher number of model parameters. Thus, models may describe a linear segment below an upper curvilinear segment[47] as well as symmetric and non-symmetric sigmoids.[48,49] A three-segment model accounts for a linear segment separating non-symmetric lower and upper curvilinear segments.[21,39,50] This model allows very accurate description of P_{el}/V curves of various shapes and has been used in conjunction with mechanical ventilation.[25,26,51]

1.8 Mathematical modelling of R

Classical observations showed proportionality between airway conductance, i.e. the inverse of R, and V.[52] This corresponds to a hyperbolic relationship between V and R. Later observations have shown a more complex relationship.[53] Efforts to model R in relation to V or P_{el} have been more sparse than modelling of P_{el}/V relationships.

Chapter 2

Aims

The objectives of the studies related to mechanical ventilation (papers I and II) were:

- to further develop the sinusoidal flow modulation method to allow recording and analysis of both inspiratory and expiratory limbs of P_{el}/V loops and to allow automatic recording of P_{el}/V loops from multiple PEEP levels.
- to analyse the relationships between inspiratory and expiratory static and dynamic P_{el}/V curves in healthy pigs and in a porcine ALI/ARDS model.
- to test the hypothesis that increasing lung collapse and re-expansion with decreasing PEEP can be characterized by hysteresis of the P_{el}/V loops.

The objectives of the studies in a clinical physiological lung laboratory (papers III and IV) were:

- to develop a method for measurement and mathematical characterization of P_{el}/V, P_{el}/C and P_{el}/R curves by applying sinusoidal flow modulation, body plethysmography and iterative analysis.
- to describe effects of aging on lung mechanics.
- to establish clinical reference values for the sinusoidal flow modulation method.

Chapter 3

Materials and Methods

3.1 Material

In papers I and II pigs of about 20 kg were studied. The pigs were anaesthetized, paralysed, intubated and ventilated with a ServoVentilator 900C (Siemens-Elema AB, Sweden). In paper I 10 healthy pigs were studied and in paper II 8 pigs were studied before and after induction of ALI/ARDS.

In papers III and IV 60 healthy, Caucasian never-smokers, 31 men and 29 women, evenly distributed in age between 20 and 65 years, were studied. Of 706 subjects, randomly selected and approached from the local population registry, 80 subjects responded. 21 did not fulfil health criteria. 3 subjects did not turn up and 3 subjects could not complete the study. In addition, 7 subjects with connection to the laboratory were included.

In paper III another 10 healthy, never-smokers were studied twice for analysis of reproducibility.

3.2 Porcine ALI/ARDS model (paper II)

The model used for induction of ALI/ARDS was based on surfactant perturbation with the detergent-like substance dioctyl sodium sulfosuccinate combined with large tidal volume ventilation at ZEEP and high inflation pressures.[54–56] The lungs were first made vulnerable by perturbing lung surfactant. Then, cyclic over-distension and expiratory lung collapse caused ventilator induced lung injury.

Criteria for ARDS, fulfilled under volume-controlled ventilation at ZEEP, were: $P_aO_2/F_IO_2 < 27$ kPa (200 mmHg) and an evident lower inflection point of the inspiratory P_{el}/V curve.

3.3 Sinusoidal flow modulation

Mechanical ventilation (papers I and II)

The modulated low-flow method[24,39] was amended by sinusoidal flow modulation also during the expiration following the flow-modulated inspiration. A computer controlled a Servo Ventilator 900C with respect to respiratory rate, inspiratory flow rate and expiratory pressure to achieve a sinusoidal modulation of inspiration and expiration (Figure 3.1).

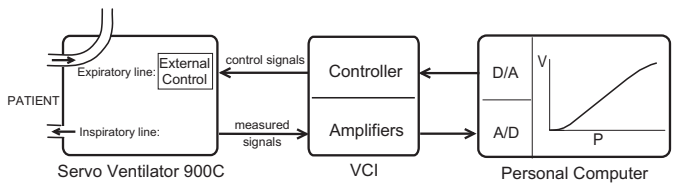

FIGURE 3.1 For automated determination of P_{el}/V curves and resistance a personal computer controlled the ServoVentilator 900C via a ventilator-computer interface (VCI) with respect to inspiratory flow rate, respiratory rate and expiratory pressure, while flow rate and expiratory pressure were measured. D/A and A/D are digital to analogue and analogue to digital converters, respectively.

To modify inspiration, signals emitted from the computer controlled, on an instantaneous basis, minute volume and respiratory rate to modify the inspiration with respect to flow rate and duration. The measured inspiratory flow signal was, within a negative feedback system, compared to the instantaneous ideal value.

To modify expiration special measures were taken because expiratory flow rate can not be directly controlled. The PEEP level was stepwise reduced in a manner resulting in a sinusoidal flow pattern. A feedback system was applied. For example, if flow rate at a certain moment was higher than intended, the pressure in the ventilator needed to be increased. Then, the difference between measured and ideal expiratory flow rate was translated into an error in ventilator pressure and PEEP was accordingly increased.

During volume-controlled inspiration adequate sinusoidal flow modulation was achieved as in previous studies[24,39] (Figure 3.2). Although the sinusoidal flow modulation was not perfect during late expiration it was adequate for its purpose to separate P_{el} from P_{res}.

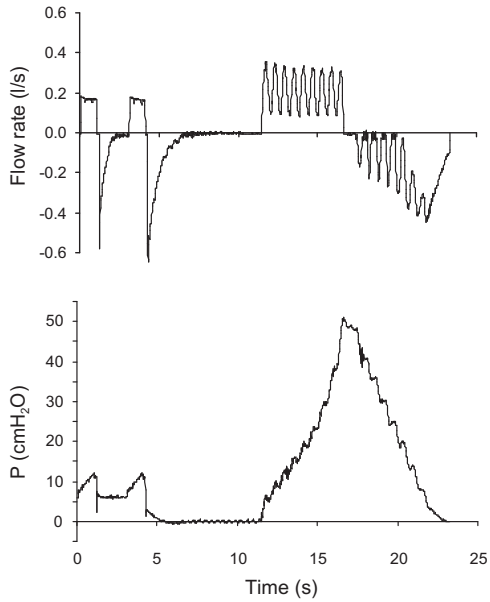

FIGURE 3.2 Flow rate and ventilator pressure (P) during recording of a dynamic P_{el}/V loop from ZEEP to 50 cmH_2O in a healthy pig.

Lung laboratory studies (papers III and IV)

The flow-regulation valve in the mouth piece comprised a silastic tube and an electric toroid motor pinching the tube. When activated through a negative feedback system, this valve regulated expiratory flow to bring it to the momentarily intended value. A series of such values were supplied from the computer to form a sinusoidal flow wave. During inspiration the valve was fully open.

The sinusoidal frequency was set at 2 Hz. Airflow rate ($\dot{V}_{ao}$) alternated between 0 and a flow rate adapted to lung size estimated from predicted total lung capacity (TLC_P). This resulted in a peak flow rate of 1.16 ± 0.07 l/s for men and 0.82 ± 0.10 l/s for women. Frequency and flow rate can be changed by the operator.

Technically the flow modulation worked as intended until physiological flow limitation commenced towards the end of deep expirations (Figure 3.3). Particularly, flow always reached close to zero in each sinusoidal cycle.

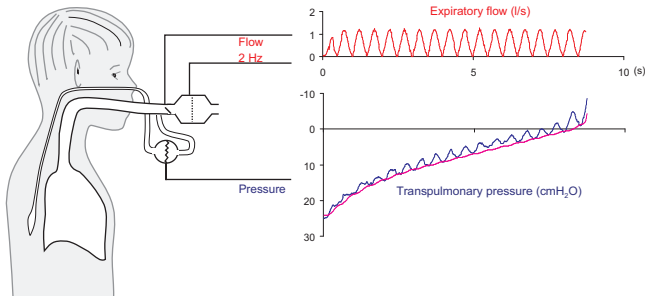

FIGURE 3.3 The sinusoidal flow signal (*red line*) and corresponding variations in transpulmonary pressure (*blue line*) during a single expiration from total lung capacity to residual volume. By iterative analysis P_{el} (*pink line*) was separated from transpulmonary pressure. The residual pressure represents resistive pressure.

3.4 Measurements and procedure (papers I and II)

In healthy pigs P_{el}/V recordings at sinusoidal flow modulation started at ZEEP and at PEEP 6 cmH_2O and ended at 20, 35 and 50 cmH_2O. Static P_{el}/V loops were recorded from ZEEP and from PEEP 6 cmH_2O to 35 cmH_2O.

In ALI/ARDS pigs multiple P_{el}/V loop recordings at sinusoidal flow modulation started at PEEP 20, 15, 10, 5 and 0 cmH_2O. All loops ended at 50 cmH_2O. Static P_{el}/V loops were recorded from ZEEP and PEEP 20 cmH_2O to 50 cmH_2O. The order between recordings was randomized.

To standardize volume history each recording was immediately preceded by a recruitment manoeuvre comprising 3 insufflations reaching 45–50 cmH_2O and lasting 15 s. The insufflations were interposed by 4 s long expirations at a PEEP level of 15–20 cmH_2O.

Recording of dynamic P_{el}/V loops

Dynamic P_{el}/V recordings are performed during continuous flow and are therefore influenced by viscoelastic phenomena (as described in section 1.5).

A computer controlled the ventilator during the full sequence of breaths comprising a P_{el}/V loop recording. An automated recording of dynamic P_{el}/V loops started with an expiration lasting 6 s at a PEEP equal to the starting pressure of the loop (Figure 3.2). The inspiratory limb was then recorded during sinusoidal

modulation of inspiratory flow. Insufflation continued until target pressure was reached. After a pause of 0.9 s, the expiratory limb was recorded while the computer sinusoidally modulated expiratory flow until starting pressure was reached.

In a fully automated sequence of breaths multiple P_{el}/V loops were recorded. 20 breaths passed between the loops recorded from lower and lower starting pressures (Figure 4.4).

Recording of static P_{el}/V loops

Static P_{el}/V recordings were based on measurement of P_{el} at truly static conditions in conjunction with a number of interrupted 'study breaths'. These recordings were therefore not influenced by viscoelastic pressure.

Recordings were performed using a computer controlled automatic flow-interruption method.[34, 57] In order to achieve static conditions and to suppress heart artefacts P_{el} was for each study breath measured as mean pressure over a complete heart cycle 3 s after flow interruption. For P_{el}/V curves recorded at PEEP and ZEEP 15 and 20 study breaths, respectively, were used for each of the inspiratory and expiratory P_{el}/V curves. Each study breath was separated by three ordinary breaths.

Each static P_{el}/V curve takes several minutes to record, since only one measurement point is obtained for each interrupted breath.

Volume alignment

The P_{el}/V curves recorded from ZEEP and PEEP at each condition were aligned at the end-expiratory volume of the ordinary breath preceding each measurement. The volume scale of P_{el}/V recordings from ZEEP and PEEP refers to the elastic equilibrium volume reached after a prolonged expiration at ZEEP.

As the complete dynamic P_{el}/V loop were recorded in immediate sequence a particular volume alignment of its limbs was not needed. Static inspiratory and expiratory P_{el}/V curves were recorded separately, implying that volume alignment was necessary. This lead to errors, which for individual pigs were not negligible.

Histopathological examination

After the experiments the lungs of the ALI/ARDS pigs were removed and 5 μm thick whole lung sections from the left lung were histopathologically examined.

3.5 Measurements and procedure (papers III and IV)

Measurements were performed with the subject sitting in a pressure-compensated, volume-displacement body plethysmograph fulfilling high technical requirements.[58] An oesophageal balloon (balloon length 10 cm, VIASYS Healthcare GmbH) was placed in the distal third of the oesophagus and filled with 0.5 ml air. An occlusion test was performed to verify determination of pleural pressure change to within ± 5%.[59]

The subjects breathed through a mouthpiece, a pneumotachograph measuring flow at airway opening ($\dot{V}_{ao}$), a flow regulator and two tubes connecting to room air. Box flow rate ($\dot{V}_{box}$) was integrated to obtain subject volume change. Pressure at airway opening (P_{ao}) and P_L were measured. P_L equals the difference between P_{ao} and oesophageal pressure (P_{oe}) ($P_L = P_{ao} - P_{oe}$).

Total lung capacity (TLC), vital capacity (VC), residual volume (RV), FRC and P_{el} at TLC ($P_{el,TLC}$) were first determined using the same body plethysmograph. Lung mechanics was then studied. The subjects inspired nearly to TLC and then exhaled towards RV, maintaining P_{ao} at 10–20 cmH_2O for as long as possible while $\dot{V}_{ao}$ was modulated, either into sinusoidal or square waves. Then, after about two tidal breaths, TGV was measured. Recordings with oesophageal contractions or improper patient cooperation were discarded. Three satisfactory recordings of each method were stored for analysis. The order between the sets of measurements with the sinusoidal flow modulation method ($\dot{V}$sine method) and the square wave flow modulation method ($\dot{V}$square method) was randomized.

For the $\dot{V}$sine method the same recordings were used for the P_{el}/V and P_{el}/R diagram. Expiratory flow and P_L during a sinusoidal expiration is illustrated in Figure 3.3.

For the $\dot{V}$square method the P_{el}/R diagram was first measured at a standardized flow rate alternating between 0 and 1.1 l/s for periods of 0.35 s and 0.3 s, respectively. The P_{el}/V diagram was then, together with measurement of TGV, measured at a flow rate alternating between 0 and 0.2×VC l/s (VC in litres) for periods of 0.5 s with the aim of recording about 10 measurement points during each deep expiration.

Although P_{el} was measured at zero flow with the $\dot{V}$square method the value does not refer to truly static conditions, because the pause at zero flow was too short for full decay of viscoelastic pressure. In this aspect the $\dot{V}$sine and the $\dot{V}$square methods are nearly equivalent.

A trig signal recorded from a single lead ECG was fed to the computer as a basis for heart artefact correction of recordings with the $\dot{V}$sine method.

P_L, P_{ao}, $\dot{V}_{ao}$ and $\dot{V}_{box}$ were sampled with a personal computer. Along with lung volume data, determined with body plethysmography, this information was transferred to a spreadsheet (Excel 2002) in a personal computer operating under

Windows (Microsoft Corporation, Redmond Washington, USA).

Heart artefact correction

Recordings with the $\dot{V}$sine method may optionally be corrected for heart artefacts affecting the P_L signal. During tidal breathing P_L, $\dot{V}_{ao}$ and an R wave trig impulse from ECG were registered over a number of breaths. The heart artefact was by averaging extracted from P_L using the trig impulse.

In recording of sinusoidal expirations the heart artefact was subtracted from recorded P_L, starting at the trig impulse.

3.6 Mathematical model for the P_{el}/V curve (papers I-IV)

To characterize the P_{el}/V curve a 6-parameter non-symmetric sigmoid model allowing for a linear segment in between a lower and an upper non-linear segment was used[21,50] (Figure 3.4). In papers III and IV P_{el} was described as a function of volume in an equation equivalent to the one introduced by Svantesson et al.[21,50] (Equation 3.1).

$$\left.\begin{array}{l}
\text{For } V<V_{LIP}: \\
P_{el} = P_{LIP} - (V_{LIP} - V_{min}) \times \frac{(P_{UIP}-P_{LIP})}{(V_{UIP}-V_{LIP})} \times \ln \frac{(V_{min}-V_{LIP})}{(V_{min}-V)} \\
\\
\text{For } V_{LIP} \leq V < V_{UIP}: \\
P_{el} = P_{LIP} + (V - V_{LIP}) \times \frac{(P_{UIP}-P_{LIP})}{(V_{UIP}-V_{LIP})} \\
\\
\text{For } V \geq V_{UIP}: \\
P_{el} = P_{UIP} + (V_{max} - V_{UIP}) \times \frac{(P_{UIP}-P_{LIP})}{(V_{UIP}-V_{LIP})} \times \ln \frac{(V_{max}-V_{UIP})}{(V_{max}-V)}
\end{array}\right\} \quad (3.1)$$

The linear segment starts at the lower inflection point (LIP) and ends at the upper inflection point (UIP). The values of pressure and volume defining the LIP and the UIP (P_{LIP}, V_{LIP}, P_{UIP} and V_{UIP}) represent four out of six parameters characterizing the P_{el}/V curve. The remaining two parameters (V_{min} and V_{max}) represent the volume asymptotes of the extrapolated non-linear segments. The equation describing the P_{el}/V curve implies that compliance is constant over the linear segment (C_{LIN}). Below the LIP and above the UIP, compliance falls linearly with volume to reach a value of zero at V_{min} and at V_{max}.

The expression $(P_{UIP} - P_{LIP})/(V_{UIP} - V_{LIP})$ in Equation 3.1 corresponds to elastance over the linear segment (E_{LIN}) and is equivalent to $1/C_{LIN}$. In the

equivalent equation in papers I and II $1/C_{LIN}$ was used. The same mathematical model was used to characterize all P_{el}/V curves.

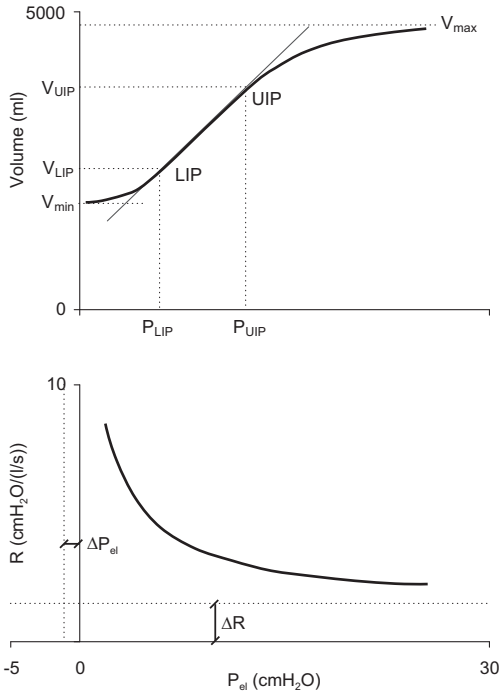

FIGURE 3.4 *Upper panel*: A P_{el}/V curve from a healthy subject (thick line). The linear segment between the lower and upper inflection points (LIP and UIP) is elucidated by its extrapolation (thin line). The six parameters describing the P_{el}/V curve are illustrated by interrupted lines. *Lower panel*: The coefficients ΔR and ΔP_{el} (interrupted lines) allow the hyperbolic P_{el}/R curve (thick line) to be displaced along the R axis and P_{el} axis, respectively.

Several mathematical models have been proposed for modelling of P_{el}/V curves. The upper segment in our model corresponds to the 3-parameter exponential model introduced by Salazar and Knowles,[46] implying that C falls linearly with increasing V over this segment. Already in 1968 Fry proposed a 5-parameter non-symmetric sigmoid model applicable for different physiological relationships, including P_{el}/V curves.[49] In 1970 Bolton underlined the sigmoid character of P_{el}/V curves.[60] In 1978 Murphy et al.[61] showed that Fry's model accurately

fitted a P_{el}/V curve comprising two segments. When analysis was applied to data depicting a typical three-segmental P_{el}/V curve the fit was less accurate. Fry's model has sparsely been applied to P_{el}/V curves. Despite the potential usefulness of Fry's model allowing modelling of non-symmetrical sigmoids, the 4-parameter sigmoid model with two symmetrical segments proposed by Venegas et al. is widely used.[48] A P_{el}/V curve often displays a linear segment below an upper curvilinear segment. These two segments can be modelled by a non-continuous 5-parameter equation.[47] To describe a P_{el}/V curve with a linear segment in between two non-symmetrical curvilinear segments a 6-parameter model is needed.[21,39,50] Such a model fulfilled our requirements by allowing very accurate description of P_{el}/V curves of various shapes. It has been used in conjunction with mechanical ventilation.[25,26,51]

In order to illustrate the nature of the models of Fry,[49] Venegas et al.[48] and Svantesson et al.[50] (the '3-segment model', Equation 3.1) a P_{el}/V curve with three segments recorded with the flow-regulator method[32] was chosen for analysis (Figure 3.5). For all three models an iterative parameter estimation was used minimizing the sum of squared differences. C was calculated as the derivatives of the P_{el}/V equations.

C plotted against V depicts model differences in that the model of Venegas is strictly symmetrical around the peak value of C (Figure 3.5, upper right panel). The 3-segment model according to Equation 3.1 shows a middle linear segment with constant C. Above and below this segment C decreases at different rates relative to volume illustrating that the upper and lower segments are non-symmetrical. In this example Fry's model showed only a slight asymmetry around the maximum C value. Notably, depending on which model is used, C at a particular V will be grossly different.

Returning to the P_{el}/V diagram one observes that the symmetrical nature of Venegas' model and the absence of a linear segment makes it impossible to describe the shape of the P_{el}/V curve in detail. The 3-segment model closely reproduces the measured P_{el}/V points. The fit of Fry's model is intermediate. The differences between the models are reflected by the R^2 values, which were 1.000 for the 3-segment model, 0.997 for Fry's model and 0.995 for Venegas' model. R^2 values of this magnitude are often interpreted as signs of excellent model qualities. According to the present example such conclusions may represent over-interpretation with respect to capacity to reflect details in shape. Notably, the quality of curve fitting is closely related to the number of model parameters. An unwarranted high number of model parameters lead to over-determination in the sense that features not related to biological phenomena, such as artefacts, may be described by the model.

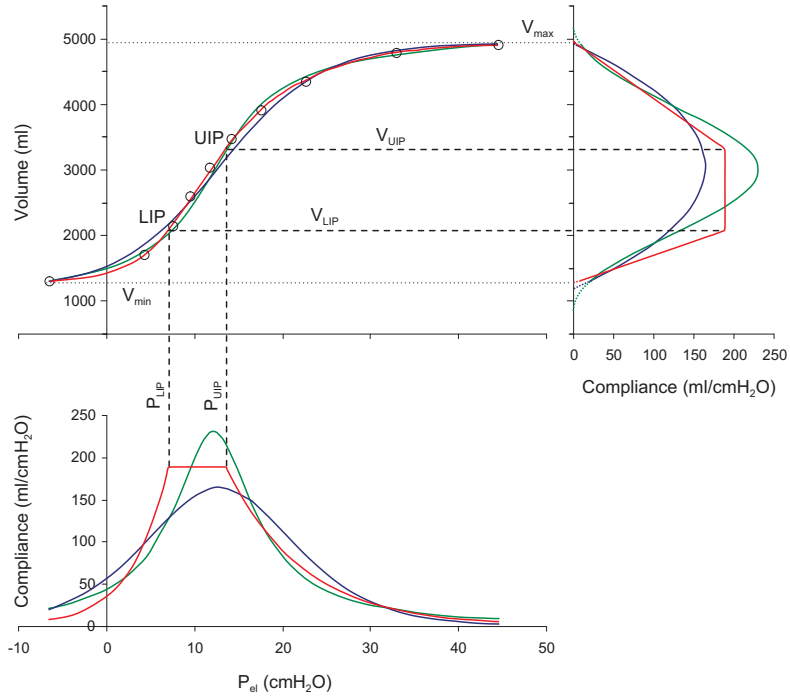

FIGURE 3.5 *Upper left panel* shows the fit to measured P_{el}/V points of the P_{el}/V models of Fry[49] (green line), Venegas et al.[48] (blue line) and Svantesson et al.[50] (red line). *Upper right panel* and *lower panel* show corresponding compliance plotted against volume and P_{el}, respectively. V_{LIP}, P_{LIP}, V_{UIP}, P_{UIP}, V_{min} and V_{max} are parameters used in Svantesson's model (Equation 3.1).

Numerous observations in both the lung laboratory and in intensive care show that a significant part of the P_{el}/V curve is linear and that it is sigmoid. The upper and lower segments represent different physiological phenomena. Therefore, there is no reason to assume that the upper and lower segments are symmetrical. The 6-parameter 3-segment model describes a non-symmetrical sigmoid with a linear segment and has no superfluous degree of freedom. Accordingly, it is not in general over-determining P_{el}/V curves.

3.7 Mathematical model for resistance

Animal studies (papers I and II)

R of the respiratory system was considered constant during inspiration but was during expiration allowed to increase at low lung volume as observed by Jonson et al.:[45]

$$R = R_0 + R_1 \times V \tag{3.2}$$

During inspiration R_1 was zero. During expiration, R_1 was zero or negative.

Lung laboratory studies (papers III and IV)

For mathematical characterization of the P_{el}/R curve a 3-parameter model based on amendments to the classical hyperbolic relationship was used:

$$R = \Delta R + \frac{1}{k \times (P_{el} - \Delta P_{el})} \tag{3.3}$$

ΔR and ΔP_{el} represent the asymptotes towards which the ends of the hyperbolic P_{el}/R curve approach and allow displacement of this curve along the R axis and P_{el} axis, respectively (Figure 3.4). The higher the value of *k* the more abrupt is the increase in R towards infinity when P_{el} approaches ΔP_{el} (Figure 3.6).

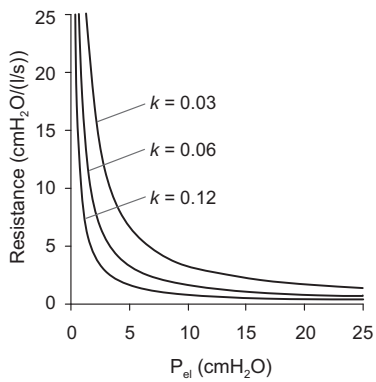

FIGURE 3.6 Varying hyperbolic P_{el}/R relationships at different values of *k*, when ΔR and ΔP_{el} are zero.

This model was used for recordings with the $\dot{V}$sine method. The sparsity and scatter of information obtained with the $\dot{V}$square method motivated that R was manually analysed by an experienced technician.

3.8 Iterative parameter estimation

P_{el} and P_{res} are partitions of P_{tr} or P_L (Equation 3.4).

$$P_{tr} \text{ or } P_L = P_{el} + P_{res} = P_{el} + R \times \dot{V} \quad (3.4)$$

For recordings at sinusoidal flow modulation (papers I-IV) P_{el} and R were functions of parameters as described above (Equations 3.1 and 3.2 or Equations 3.1 and 3.3).

P_{res}, with its sinusoidal variations, was separated from P_{el} in an iterative analysis of P_L or P_{tr} and flow rate yielding the P_{el}/V and the P_{el}/R curve. In the iterative analysis the parameters were adjusted according to the principle of Newton-Raphson until the sum of squared differences between measured and calculated P_L or P_{tr} reached a minimum.

The mathematical description of for example a P_{el}/V curve allows compilation of data and comparisons between different groups or conditions. The parameters in themselves reflect complex physiology. In general, the value of a particular parameter conveys information that is difficult to interpret.[51]

For recordings with the V̇square method, the sum of squared differences between measured P_{el} and P_{el} calculated according to Equation 3.1 was minimized.

3.9 Data analysis following iterative parameter estimation

Papers I and II

Hysteresis, defined as the volume difference between the inspiratory and the expiratory limb of a P_{el}/V loop (ΔV_{hyst}), was calculated over the whole P_{el} range. De-recruitment volumes (ΔV_{DER}) were measured as the difference between the beginning of an inspiratory dynamic P_{el}/V curve from PEEP and the inspiratory dynamic ZEEP curve (1, 2, 3 and 4 in Figure 4.4, page 27).

Papers III and IV

The complete P_{el}/C curve was calculated as the derivative of the P_{el}/V curve. C over the P_{el} interval 5–15 cmH_2O ($C_{5\text{-}15}$) was also calculated.

Based on the assumption that small and large lungs are of similar quality, values for V and C at given values of P_{el} were in paper IV normalized by calculating V/TLC_P and C/TLC_P. Calculation of reference values and studies of age dependence of V and C were based on Equations 3.5 and 3.6:

$$a)\ V/TLC_P = v_1 + v_2 \times age \qquad b)\ V = (v_1 + v_2 \times age) \times TLC_P \quad (3.5)$$

$$a)\ C/TLC_P = c_1 + c_2 \times age \qquad b)\ C = (c_1 + c_2 \times age) \times TLC_P \tag{3.6}$$

Classical observations indicate that the reciprocal of R, conductance, is roughly proportional to lung size.[52,62] When conductance, measured at a flow rate standardized to lung size, was normalized to lung size and related to P_{el}, rather than to V, differences between healthy subjects decreased.[62] To characterize resistive properties our method was based on this knowledge. To account for differences in TLC_P, age dependence of R at particular values of P_{el} was studied based on Equation 3.7:

$$a)\ R \times TLC_P = r_1 + r_2 \times age \qquad b)\ R = (r_1 + r_2 \times age)/TLC_P \tag{3.7}$$

v_1, v_2, c_1, c_2, r_1 and r_2 were obtained from regression analyses performed according to Equations 3.5 a, 3.6 a and 3.7 a. These coefficients were used to calculate predicted values for V, C and R at different values of P_{el} (Equations 3.5 b, 3.6 b and 3.7 b).

3.10 Statistical analysis

Results are presented as average values ± standard deviation (SD) or standard error of the mean (SEM) when the interest is focused on differences between groups. When regression analyses were performed results were presented as the equations ± 1 residual standard deviation (RSD). Bland-Altman plots were used to compare methods.[63] Comparisons were made with *t*-test or when indicated with 2-way ANOVA (Microsoft® Excel 97, Microsoft, Redmond, WA, US). Reproducibility of methods (paper III) were presented as median, 75^{th} and 95^{th} percentile and comparisons were made with Wilcoxon signed rank test. Regarding the relationship between body height and TLC_P (paper IV) a non-linear regression analysis was performed. In other circumstances of regression analyses linear regressions were performed. $P<0.05$ indicated statistical significance.

Chapter 4

Results and Comments

4.1 ALI/ARDS model (paper II)

After post mortem removal, all lungs were atelectatic except in the upper ventral regions. Histopathology showed modest changes compatible with an early stage of ALI/ARDS. Leukocyte infiltration and epithelial damage were found in bronchioles. In alveolar walls oedema, hyaline membranes and infiltration of neutrophil granulocytes were observed.

Poor oxygenation at ZEEP, lung collapse at lower PEEP levels observed in multiple inspiratory P_{el}/V curves and high P_{LIP} values in the inspiratory P_{el}/V curves from ZEEP were consistent with ALI/ARDS. A change in P_{el}/V curve shape was, for both inspiration and expiration, paralleled by large differences in C plotted against P_{el}. Unchanged C calculated over the P_{el} range 0–50 cmH_2O, good oxygenation at a PEEP of 20 cmH_2O and modest histopathological changes suggested that the aberrations in P_{el}/V relationships reflected functional rather than morphological perturbations as in an early stage of ALI/ARDS.

4.2 Resistance (papers I and II)

A model with constant inspiratory R was found adequate. Inspiratory R increased significantly from 2.6 ± 0.8 $cmH_2O/(l/s)$ at health to 5.0 ± 1.7 $cmH_2O/(l/s)$ in ALI/ARDS (paper II).

Expiratory R increased during expiration, particularly in ALI/ARDS. In recordings from 50 cmH_2O to ZEEP expiratory R increased significantly from 2.8 ± 2.4 $cmH_2O/(l/s)$ at the beginning of expiration to 6.3 ± 4.0 $cmH_2O/(l/s)$ at its end ($p=0.01$). Accordingly, modelling of the variation in R during expiration increased the accuracy in determination of dynamic P_{el}/V curves.

4.3 P_{el}/V loops (papers I and II)

Differences between static and dynamic P_{el}/V loops

Findings discussed in this paragraph were, in principle, similar in healthy pigs (paper I) and in pigs with ALI/ARDS (paper II). Phenomena related to lung collapse/re-expansion were more pronounced in ALI/ARDS.

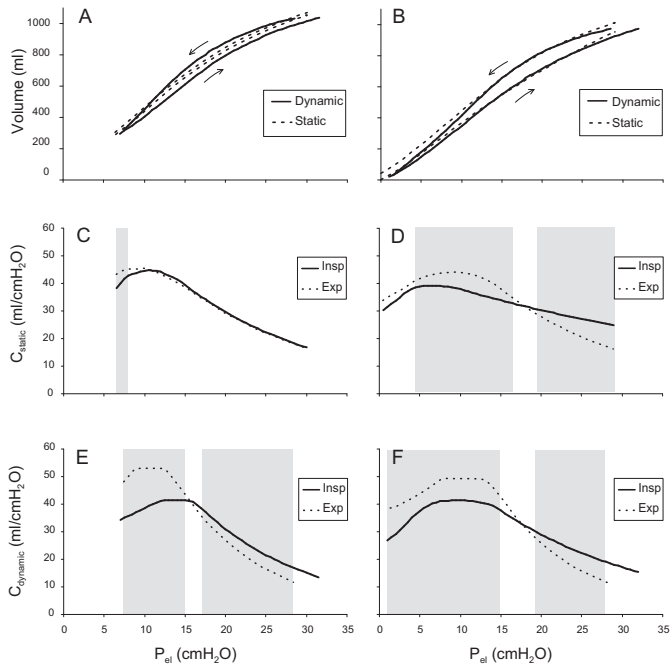

FIGURE 4.1 Averaged results in healthy pigs for static and dynamic recordings from PEEP and ZEEP are shown in *left* and *right panels*, respectively. *Grey area background* indicate the ranges of pressure over which compliance differ significantly ($p<0.05$).

Static P_{el}/V loops recorded from PEEP showed no hysteresis and no significant difference between inspiratory and expiratory C (Figure 4.1 A and C). This indicated that static P_{el}/V loops recorded from PEEP were influenced neither by surface tension hysteresis nor by lung collapse/re-expansion. Static P_{el}/V loops from ZEEP and dynamic P_{el}/V loops from ZEEP and PEEP showed hysteresis (Figure 4.1 A and B). As a result, expiratory C was significantly lower than inspiratory at the beginning of expiration and significantly higher at the latter

part of expiration (Figure 4.1 D, E and F). As static P_{el}/V loops from PEEP showed no hysteresis, the hysteresis observed in dynamic P_{el}/V loops from PEEP is considered to reflect viscoelastic phenomena. Hysteresis in static P_{el}/V loops recorded from ZEEP and corresponding significant differences in C probably reflect lung collapse/re-expansion. In dynamic P_{el}/V loops recorded from ZEEP the summation of effects caused by viscoelastic phenomena and lung collapse/re-expansion explains the larger hysteresis. The findings confirm that even healthy pigs have a tendency to lung collapse at low PEEP levels.[64,65] The observations in Figure 4.2 are in line with re-expansion at high inspiratory pressures and lung collapse during ensuing expirations. Viscoelasticity may contribute to the pattern.

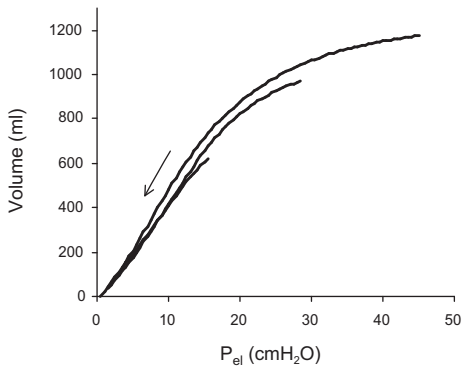

FIGURE 4.2 Averaged expiratory dynamic P_{el}/V curves from 20, 35 and 50 cmH_2O to ZEEP in healthy pigs. At common P_{el} values, curves starting at high pressures had, during the initial part of expiration, higher volume and compliance in agreement with that collapsed lung units were re-expanded at high pressures.

During the initial part of both inspiration and expiration dynamic C was significantly lower than static C at both ZEEP and PEEP as expected from build up of viscoelastic pressure (Figure 4.3 C and D).

Differences between static and dynamic P_{el}/V curves were explained by viscoelastic phenomena that influenced hysteresis. However, both static and dynamic P_{el}/V curves clearly display the tendency of lung collapse/re-expansion at low PEEP.

Multiple dynamic P_{el}/V loops in ALI/ARDS (paper II)

In multiple P_{el}/V loops, starting at lower and lower PEEP levels, volume losses representing collapse of lung units for each step of lower PEEP were observed

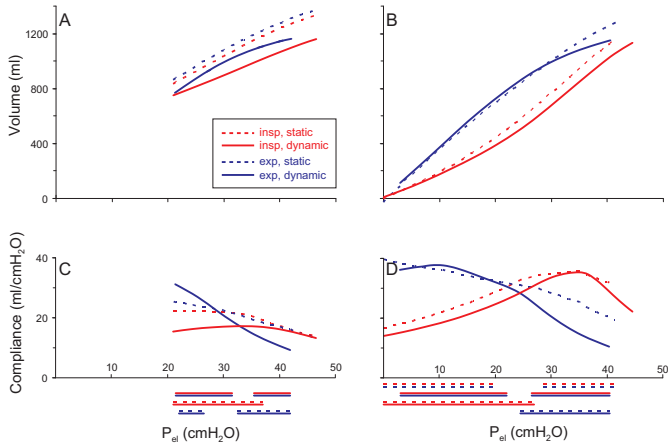

FIGURE 4.3 Averaged results in ALI/ARDS pigs for static (*interrupted lines*) and dynamic recordings (*continuous lines*) from PEEP and ZEEP are shown in left and right panels, respectively. The ranges of pressure over which compliance differ significantly ($p<0.05$) are indicated in lower panels by pairs of lines representing the two curves.

between the inspiratory limbs (*a*, *b*, *c* and *d* in Figure 4.4).

Inspiratory P_{el}/V curves were essentially parallel up to a pressure of about 20 cmH_2O, indicating that volume losses were not regained. Between 20 and 40 cmH_2O the inspiratory P_{el}/V curves approached each other implying continuing re-expansion of collapsed lung units. Re-expansion was reflected by a higher inspiratory C within the common P_{el} range (21 to 44.5 cmH_2O) for P_{el}/V curves starting at lower PEEP levels. Inspiratory P_{el}/V curves merged at about 40 cmH_2O indicating complete re-expansion. Expiratory P_{el}/V curves, all starting from 50 cmH_2O, overlapped.

4.4 Hysteresis (papers I and II)

In recordings from ZEEP to 50 cmH_2O, the volume difference between the inspiratory and expiratory limbs of dynamic P_{el}/V loops (ΔV_{hyst}) was significantly larger in ALI/ARDS compared to at health. Maximum hysteresis was observed at 17 ± 3 cmH_2O before and at 24 ± 3 cmH_2O in ALI/ARDS ($p=0.003$), indicating that higher pressures were required for re-expansion in ALI/ARDS than at health (Figure 4.5). At decreasing PEEP, ΔV_{hyst} increased, indicating continuing lung

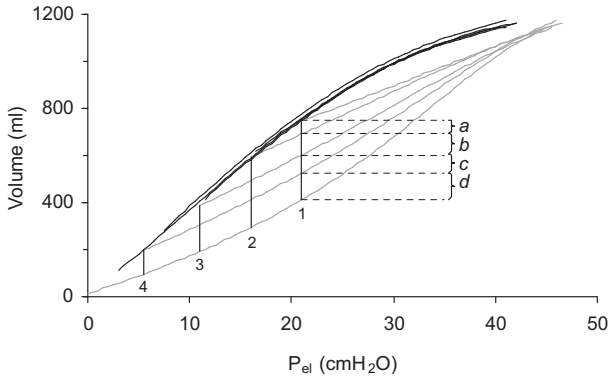

FIGURE 4.4 Averaged multiple dynamic P_{el}/V loops in ALI/ARDS pigs. Inspiratory P_{el}/V curves (*grey*) are recorded from 20, 15, 10, 5 and 0 cmH_2O. The corresponding expiratory curves (*black*), all recorded from 50 cmH_2O, overlap. The volume change caused by de-recruitment for the pressure decrements 20–15, 15–10, 10–5 and 5–0 cmH_2O are marked *a*, *b*, *c* and *d*, respectively. 1, 2, 3 and 4 denote ΔV_{DER}, i.e. volume differences between the beginnings of inspiratory P_{el}/V curves from 20, 15, 10 and 5 cmH_2O, respectively, and the inspiratory P_{el}/V curve from ZEEP.

collapse during expiration followed by re-expansion at higher pressures during the ensuing inspiration (Figure 4.4 and Figure 4.5).

One approach to the study of lung collapse/re-expansion is to measure ΔV_{hyst} of P_{el}/V loops recorded from different PEEP levels. Another approach is to study multiple inspiratory P_{el}/V curves and to measure the volume differences 1, 2, 3 and 4 in Figure 4.4 (ΔV_{DER}). In ALI/ARDS, an issue is whether the information obtained by one approach is equivalent to that of the other one. A comparison between ΔV_{hyst} and ΔV_{DER} showed no significant difference ($p=0.31$) (Figure 4.6). Each of the approaches provides additional aspects related to lung collapse/re-expansion. Further evaluation in clinical settings is motivated.

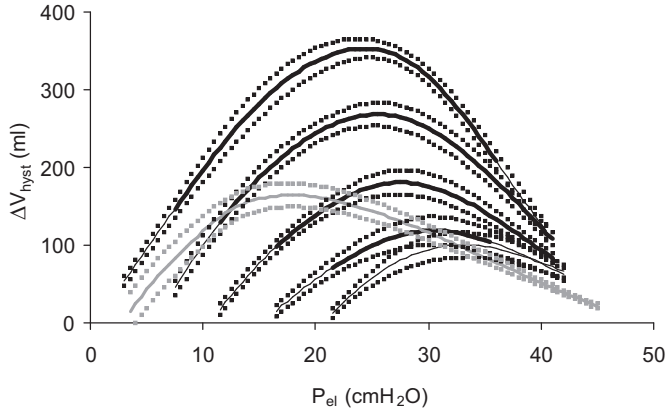

FIGURE 4.5 Hysteresis volume (ΔV_{hyst}) ± SEM of multiple dynamic P_{el}/V loops in ALI/ARDS pigs (*black lines and dots*). Heavy segments indicate that the difference from the preceding loops recorded from a higher PEEP is significant. *Grey lines and dots* show the findings at health.

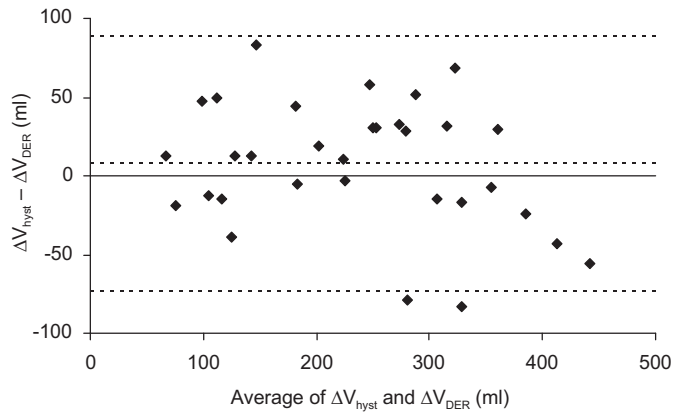

FIGURE 4.6 ΔV_{DER} and ΔV_{hyst} analysed according to Bland and Altman. ΔV_{DER} is explained in Figure 4.4. ΔV_{hyst} is the width of the P_{el}/V loop recorded from ZEEP at the same pressures. ΔV_{hyst} was 7±40 ml larger than ΔV_{DER}. The difference was not significant (p=0.31). Interrupted lines represent average difference ± 2 SD.

4.5 Lung laboratory studies (papers III and IV)

Mathematical characterization

The mathematical model for the P_{el}/V curve (Equation 3.1) and for the P_{el}/R curve (Equation 3.3) resulted in a good visual fit between measured and calculated P_L. The P_{el}/V curve was well described by the sigmoid model. All 60 subjects had an upper segment with C decreasing towards higher V. 54 of them had a middle linear segment with constant C. A lower segment with C decreasing towards lower V was observed in 13 subjects, mostly younger ones.

A mathematical description of the P_{el}/V curve allows calculation of the complete P_{el}/C curve, which conveys more detailed information than a single value of C calculated over a certain pressure or volume interval.

Comparison of the $\dot{V}sine_{corr}$ method and the $\dot{V}square$ methods (paper III)

A comparison of values obtained with the $\dot{V}sine$ method with heart-artefact correction ($\dot{V}sine_{corr}$ method) and the $\dot{V}square$ method is shown in Figure 4.7. V measured at P_{el} values between 5 and 15 cmH_2O were equal for the two methods. $C_{5\text{-}15}$ was for the $\dot{V}sine_{corr}$ method 6 ± 17 ml/cmH_2O lower ($p=0.02$), corresponding to 2.6% of the average. R at P_{el} 10 cmH_2O did not differ between the methods. Differences between methods in V and C were equally distributed at all average values (Figure 4.7, upper right panels). Differences in R at P_{el} 10 cmH_2O were proportional to the average of the methods (Figure 4.7, lower right panel).

Comparison of the $\dot{V}sine_{corr}$ method and the $\dot{V}sine_{uncorr}$ methods (paper III)

In the ten subjects studied twice, values of V, C and R obtained with the $\dot{V}sine_{corr}$ method and with the $\dot{V}sine$ method without heart artefact correction ($\dot{V}sine_{uncorr}$ method) showed no significant difference within the compared P_{el} range 5–25 cmH_2O.

Reproducibility of the $\dot{V}sine$ and $\dot{V}square$ methods (paper III)

For analysis of reproducibility absolute differences in V, C and R between measurement occasions were calculated over P_{el} ranges considered clinically most relevant. For V the difference over the P_{el} range 5–25 cmH_2O was used. For C the difference in $C_{5\text{-}15}$ and for R the difference over P_{el} 5–10 cmH_2O were used.

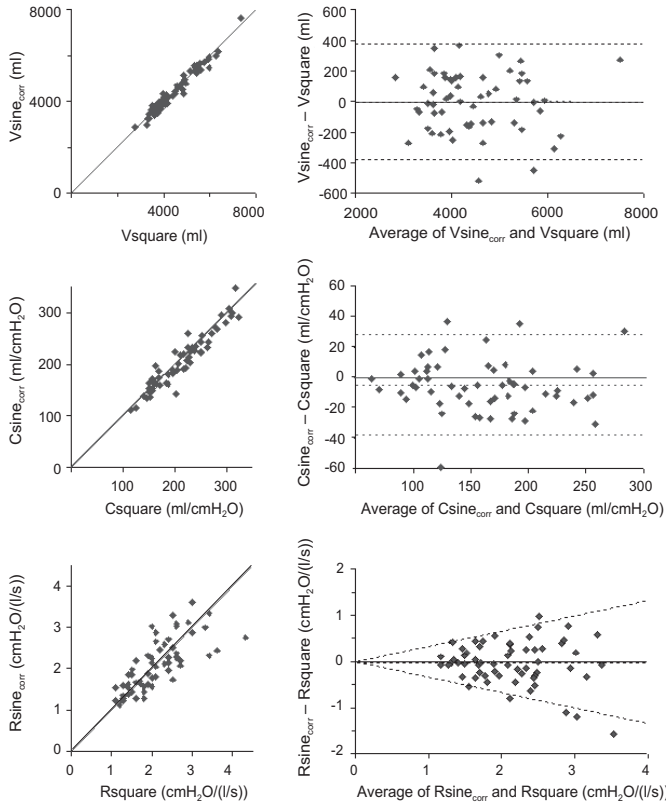

FIGURE 4.7 Volume at P_{el} 10 cmH_2O ($Vsine_{corr}$, Vsquare), compliance over P_{el} 5–15 cmH_2O ($Csine_{corr}$, Csquare) and expiratory lung resistance at 10 cmH_2O ($Rsine_{corr}$ and Rsquare) measured with the $\dot{V}sine_{corr}$ and $\dot{V}$square method, respectively, plotted with the identity line (*left panel*) and analysed according to Bland and Altman (*right panel*). Interrupted lines represent for volume and compliance the average difference ±1.96 SD and for resistance the 95% confidence interval.

Reproducibility did not show any significant difference between the $\dot{V}sine_{corr}$, $\dot{V}sine_{uncorr}$ and $\dot{V}square$ methods ($p>0.05$, Wilcoxon signed rank test)(Table 4.1).

TABLE 4.1
Reproducibility of the $\dot{V}sine_{corr}$, $\dot{V}sine_{uncorr}$ and $\dot{V}square$ methods

	$\dot{V}sine_{corr}$	$\dot{V}sine_{uncorr}$	$\dot{V}square$
$\lvert\Delta V\rvert$ (*ml*)			
Median	130 (2.3%)	140 (2.4%)	118 (1.9%)
75th percentile	168 (2.5%)	169 (2.9%)	175 (3.1%)
95th percentile	358 (7.9%)	334 (6.5%)	303 (7.3%)
$\lvert\Delta C_{5\text{-}15}\rvert$ (*ml/cmH_2O*)			
Median	8 (4.5%)	13 (5.3%)	17 (7.2%)
75th percentile	14 (7.1%)	18 (8.6%)	25 (11.4%)
95th percentile	19 (8.6%)	22 (9.9%)	42 (18.1%)
$\lvert\Delta R\rvert$ (*cmH_2O/(l/s)*)			
Median	0.17 (9.3%)	0.18 (10.1%)	0.15 (6.4%)
75th percentile	0.35 (16.3%)	0.27 (12.6%)	0.29 (9.7%)
95th percentile	1.55 (39.7%)	1.37 (35.2%)	0.35 (16.3%)

Absolute difference between measurement occasions in volume over P_{el} 5–25 cmH_2O ($\lvert\Delta V\rvert$), in compliance over P_{el} 5–15 cmH_2O ($\lvert\Delta C_{5\text{-}15}\rvert$) and in resistance over P_{el} 5–10 cmH_2O ($\lvert\Delta R\rvert$).
Values in parenthesis represent the differences as percentage of average volume, compliance and resistance over the same P_{el} ranges.

Figure 4.8 shows the two P_{el}/V curves recorded with the $\dot{V}sine_{corr}$ method on different days in 10 healthy subjects.

Heart-artefact correction did not improve reproducibility of the $\dot{V}sine$ method. An explanation may be that the mathematical modelling of the P_{el}/V and the P_{el}/R curves restrain the degrees of freedom to physiologically reasonable shapes of the curves. Accordingly, random influences are 'filtered away'.

Further comments to paper III

From a shorter procedure using the $\dot{V}sine$ method P_{el}/V and P_{el}/R curves were obtained with the same quality as with the more time consuming $\dot{V}square$ method. In addition, the $\dot{V}sine$ method offers mathematical characterization of P_{el}/V, P_{el}/C and P_{el}/R curves. In healthy subjects we found no benefit of heart-artefact

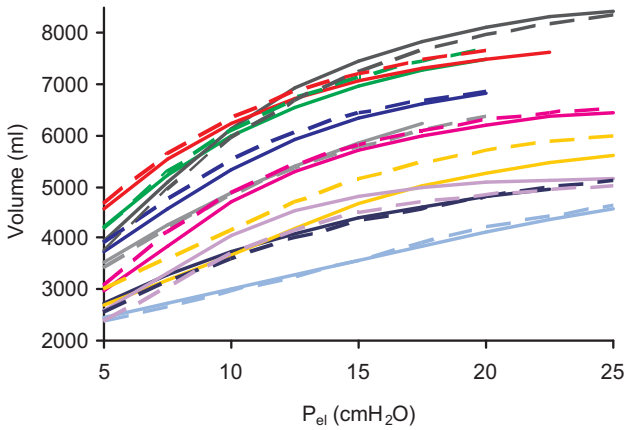

FIGURE 4.8 P_{el}/V curves recorded on measurement day 1 (*continuous lines*) and 2 (*interrupted lines*) with the $\dot{V}sine_{corr}$ method. Each colour represents one subject.

correction. In patients ventilated for critical lung disease, heart artefacts in P_{tr} were five times larger than in humans without lung disease.[66] Whether recordings in patients, who may have larger heart artefacts, are improved by heart-artefact correction needs to be studied.

Effects of aging on lung mechanics and reference values (paper IV)

As in most previous materials TLC showed no significant age dependence. A power equation (Equation 4.1), common for men and women, adequately described TLC_P [litre] as a function of body height [meter]:

$$TLC_P = 1.12 \times body\ height^{3.129} \pm 0.66 \quad (4.1)$$

To normalize for lung size, TLC_P in Equations 3.5, 3.6 and 3.7 was calculated from Equation 4.1.

TLC_P based on our own material has the advantages that TLC was measured with the same equipment and technique as volumes in the P_{el}/V curves and that problems related to different selections when using other reference equations were avoided. After normalization of P_{el}/V, P_{el}/C and P_{el}/R curves for lung size (Equations 3.5, 3.6 and 3.7) no differences between sexes were observed. Merging

men and women rendered power to the statistical analysis. A relation between TLC and body height, common for men and women, was in a similar context described by Knudson et al.[11] In small groups of men and women, when lung size was taken into account, Gibson et al. and Knudson et al. found no sex differences in elastic properties of human lung.[10,11]

When TLC instead of TLC_P is used for normalizing, disturbed neuromuscular function becomes a confounding factor. Reduced TLC due to reduced muscle strength cause a shift of P_{el}/V curves normalized to TLC towards lower P_{el}.[10] In addition, pathology in P_{el}/V curves normalized to TLC may be concealed if TLC is increased or decreased due to fibrosis or emphysema.[2]

In the studied P_{el} range, 5 to 25 cmH_2O, regression analyses showed that V and C were proportional to TLC_P ($p<0.001$) supporting analysis according to Equations 3.5 and 3.6. Figure 4.9 shows predicted P_{el}/V, P_{el}/C and P_{el}/R curves for persons of varying age, all with a TLC_P of 6.3 litres. To calculate reference data of clinical utility, coefficients for reference equations for P_{el}/V, P_{el}/C and P_{el}/R curves normalized to TLC_P are presented in paper IV.

V/TLC_P increased significantly with increasing age for all P_{el} values up to 20 cmH_2O. Also the width of the normal range for the P_{el}/V curve increased significantly with age ($p=3\times10^{-10}$) (Figure 4.10). This might reflect that the rate of loss of elastic recoil with age differs among individuals, just as it does in the skin. Reciprocally, the loss of P_{el} at different volumes was studied. $P_{el,TLC}$ was equal in men and women and decreased with age (Equation 4.2).

$$P_{el,TLC} = 45.6 - 0.28 \times age \pm 7.7\ cmH_2O \tag{4.2}$$

The decrease in P_{el} with age was largest at high degrees of lung distension as previously observed[10,12] (Table 4.2). The rate of elastic recoil loss with age was similar to that found by Turner et al. and Gibson et al., but higher than that found by Knudsen et al.[10–12] Knudsen et al. excluded subjects with FEV%<75%. Roughly about 50% of a healthy population at an age of 60 years have FEV% <75%. Therefore, a selection bias towards older subjects with constitutionally high or better-preserved P_{el} must be anticipated in the study of Knudson et al. In paper IV, subjects over 65 years of age were not included due to the risk of selection bias towards a particularly active and well-being population.

$C_{5\text{-}15}$ [ml/cmH_2O] normalized to TLC_P [litres] ($C_{5\text{-}15}/TLC_P$) was equal in men and women and decreased with increasing age (Equation 4.3).

$$C_{5-15}/TLC_P = 38.7 - 0.13 \times age \pm 5.0 \tag{4.3}$$

C/TLC_P decreased with increasing age at $P_{el} \geq 10$ cmH_2O, but increased with increasing age at P_{el} 5 cmH_2O.

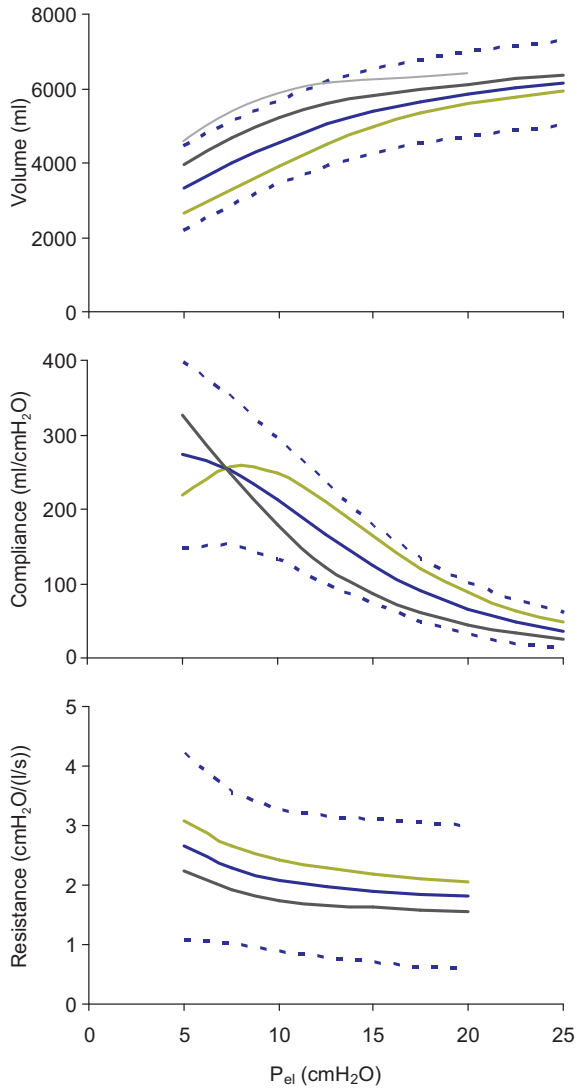

FIGURE 4.9 Predicted P_{el}/V, P_{el}/C and P_{el}/R curves at the age of 20 (*green*), 47.5 (*blue*) and 65 years (*black*), all with a TLC_P of 6.3 litres. *Interrupted blue lines* show normal ranges for a 47.5 year old person. For discussion only, the *thin grey line* indicates a hypothetical P_{el}/V curve, based on extrapolation of the reference equation to an 87 year old person.

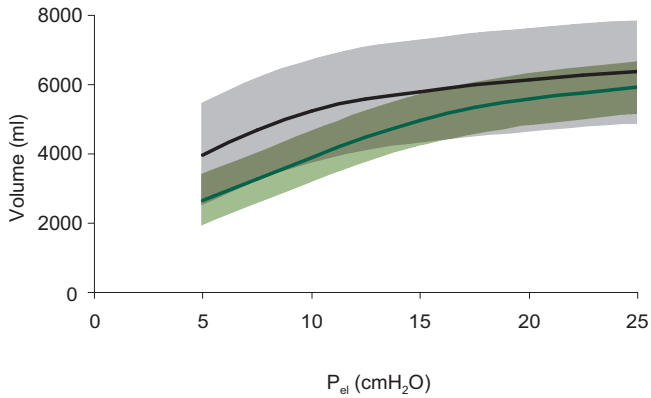

FIGURE 4.10 Predicted P_{el}/V curve and normal range for a 20 year old person (*green*) and a 65 year old person (*black and grey*) with a TLC_P of 6.3 litres.

TABLE 4.2
Decrease in P_{el} from 20 to 65 years of age

	TLC	$TLC_{P(90\%)}$	$TLC_{P(80\%)}$	$TLC_{P(70\%)}$
Total decrease in P_{el} (cmH_2O)	12.6	8.0	6.3	5.6
Yearly decrease in P_{el} ($cmH_2O/year$)	0.28	0.18	0.14	0.12

Decrease in P_{el} with age at measured TLC and at 90, 80 and 70% of TLC_P ($TLC_{P(90\%)}$, $TLC_{P(80\%)}$and $TLC_{P(70\%)}$, respectively).

In our material P_{el} at FRC was about 5 cmH_2O. The positive age dependence of C/TLC_P at P_{el} 5 cmH_2O confirms some previous studies in which C measured in the normal tidal-volume range tended to increase with age.[10, 13–16]

In critical lung disease, the significance of C as a factor not only reflecting distensibility of lung tissue has since long been discussed and recently reviewed.[51, 67] C is volume change (ΔV) related to change in P_{el} (ΔP_{el}):

$$C = \Delta V / \Delta P_{el} \tag{4.4}$$

ΔV constitutes not only a volume change related to a gradual change in degree of distension of open lung units ($\Delta V_{distension}$). Another partition of ΔV represents a sudden volume change when collapsed lung units are re-expanded during

inspiration or, at expiration, when gas is expulsed due to alveolar collapse. This partition is denoted ($\Delta V_{re\text{-}exp/collapse}$):

$$C = \frac{(\Delta V_{distension} + \Delta V_{re\text{-}exp/collapse})}{\Delta P_{el}} \quad (4.5)$$

In conjunction with mechanical ventilation the influence of $\Delta V_{re\text{-}exp/collapse}$ has been intensively discussed with respect to inspiratory P_{el}/V curves. Obviously, expiratory P_{el}/V curves are affected by $\Delta V_{collapse}$ when alveolar collapse occurs. The fact that collapse occurs at much lower degrees of lung distension compared to when re-expansion occurs during inspiration is a major reason for hysteresis.[23,44] Even in healthy humans alveolar collapse occurs at low degrees of lung distension, for example during anaesthesia.[50,68] Collapse occurs after a single expiration in anaesthetized healthy humans[69] and in pigs at health and in ALI/ARDS (papers I and II). Reasonably, collapse also occurs when humans actively expire towards RV. From this aspect, observations in low ranges of volume and P_{el} motivate discussion of events affecting the lowermost segment of the P_{el}/V and P_{el}/C curve (paper IV).

Below P_{el} 10 cmH_2O, complex phenomena such as airway closure and expulsion of gas from collapsing lung units may contribute to the pattern of P_{el}/C curves. If airways close towards the end of expiration, gas trapping results in flattening of the P_{el}/V curve implying decreasing C. If instead alveoli collapse, expulsion of gas will contribute to volume change and lead to an increase in C over a pressure interval corresponding to the range of closing pressure.[51] The findings in paper IV lead to the hypothesis that the former phenomenon explains the P_{el}/C pattern in younger subjects, while the latter phenomenon dominates in older subjects.

The increase in RV with age was only 69% of the increase in V at a P_{el} of 5 cmH_2O. Furthermore, younger subjects had more often a lower non-linear segment of the P_{el}/V curve over which C decreased. Together, these observations suggest that different phenomena influence RV and P_{el}/V curves in young and old subjects. In older subjects expulsion of gas from collapsing alveoli might both limit age-dependent increase of RV and conceal signs of small airway closure in the P_{el}/V curve. At certain values of P_{el}, airway dimensions are wider in older subjects, as shown by lower values of R. The wider airways may therefore in old subjects stay open at lower values of P_{el} compared with young subjects.

Previous studies provide indirect evidence of wider airway dimensions at high age.[10,70] Loss of elastic recoil of the airway itself may explain wider airways at particular values of P_{el}.[11] Considering that intrapulmonary airways are part of the three dimensional elastic pulmonary network it appears reasonable that airways, like alveoli, lose elastic recoil with age.

As shown in Figure 4.9 $R \times TLC_P$ was age dependent when related to P_{el}. When $R \times TLC_P$ was related to V rather than to P_{el} no age dependence was found.

V is an expression of dimensions of pulmonary structures, including airways. R reflects radius of airways. Therefore, age independence of R in relation to V may indicate that intrinsic recoil of the airways decreases with age to a similar extent as P_{el} decreases with age.

At $P_{el} \geq 10$ cmH_2O C was lower in older subjects (Figure 4.9). Notably, at given values of P_{el} V is higher in older subjects, implying that the elastic fibrous network is stretched closer to its maximal extension. This may explain that C related to V was age independent. This notion may be linked to observations that the collagen content per unit volume of distended lung remains unchanged with age.[71]

The hypothetical P_{el}/V curve for an 87 year old person suggests that elastic recoil at high age is very low (Figure 4.9). Considering that the loss of P_{el} appears to accelerate at high age,[72] the loss of P_{el} in the 87 year old person might even have been underestimated. Furthermore, the wide normal range of the P_{el}/V curve in elderly people means that some may have extremely low elastic recoil. In such persons, lung collapse and atelectasis formation with reduced arterial oxygenation due to shunting[73] may affect well-being, activities of daily life and even survival. This may be the case even in the absence of pulmonary disease. Particularly with respect to our aging population, further studies are motivated.

Chapter 5

Major Conclusions

Papers I and II

In mechanically ventilated pigs sinusoidal flow modulation allowed automated recording and detailed characterization of dynamic P_{el}/V loops. Compared to static P_{el}/V recording dynamic recording is much faster. Both at health and in ALI/ARDS differences between dynamic and static P_{el}/V loops were explained by viscoelastic phenomena, which contributed to hysteresis. Absence of hysteresis in static P_{el}/V loops from PEEP support previous notions that surfactant-film hysteresis contributes insignificantly to hysteresis. Hysteresis in static P_{el}/V loops from ZEEP was therefore explained by lung collapse/re-expansion.

In ALI/ARDS hysteresis, defined as the volume difference at a certain P_{el} between the expiratory and inspiratory limb of a P_{el}/V loop provided similar information about lung collapse and re-expansion as multiple inspiratory P_{el}/V curves recorded from varying PEEP levels.

Paper III

With the $\dot{V}$sine method P_{el}/V and P_{el}/R curves were obtained with the same quality as with the more time consuming $\dot{V}$square method. In addition, the $\dot{V}$sine method offers mathematical characterization of P_{el}/V, P_{el}/C and P_{el}/R curves facilitating scientific analysis, storage of data and comparisons in conjunction of clinical follow up. In healthy subjects we found no benefit of heart-artefact correction.

Paper IV

An important result is that representative reference values for P_{el}/V, P_{el}/C and P_{el}/R curves make the V̇sine method clinically useful. Previous studies have reported different rates of decline in P_{el} with age. Our findings agree with the higher rates of elastic recoil loss with age. The width of the normal range for the P_{el}/V curve increased with age, indicating individual rate of aging comparable to that of the skin. At P_{el} 5 cmH_2O, roughly corresponding to FRC, compliance increased with age as previously observed. At P_{el} values $\geq$10 cmH_2O compliance decreased with age. The findings suggest that the lower part of the P_{el}/V curve in old subjects is influenced by collapsing alveoli, while in younger subjects airway closure dominates. Resistance in relation to P_{el} decreased with age. When compliance and resistance were related to volume rather than to P_{el} no age dependence was observed. Accordingly, the dimension of the lung rather than the distending pressure P_{el} seems to be a determinant of compliance and resistance.

References

1. S. S. Wagers, T. G. Bouder, D. A. Kaminsky, and C. G. Irvin. The invaluable pressure-volume curve. *Chest*, 117(2):578–83, 2000.

2. B. Jonson. Pulmonary mechanics in patients with pulmonary disease, studied with the flow regulator method. *Scand J Clin Lab Invest*, 25(4):375–90, 1970.

3. E. P. Ingenito, R. B. Evans, S. H. Loring, D. W. Kaczka, J. D. Rodenhouse, S. C. Body, D. J. Sugarbaker, S. J. Mentzer, M. M. DeCamp, and Jr. Reilly, J. J. Relation between preoperative inspiratory lung resistance and the outcome of lung-volume-reduction surgery for emphysema. *N Engl J Med*, 338(17):1181–5, 1998.

4. A. N. Aggarwal, D. Gupta, D. Behera, and S. K. Jindal. Analysis of static pulmonary mechanics helps to identify functional defects in survivors of acute respiratory distress syndrome. *Crit Care Med*, 28(10):3480–3, 2000.

5. I. Brådvik, P. Wollmer, B. Simonsson, U. Albrechtsson, K. Lyttkens, and B. Jonson. Lung mechanics and their relationship to lung volumes in pulmonary sarcoidosis. *Eur Respir J*, 2(7):643–51, 1989.

6. B. Blom-Bülow, B. Jonson, and K. Brauer. Lung function in progressive systemic sclerosis is dominated by poorly compliant lungs and stiff airways. *Eur J Respir Dis*, 66(1):1–8, 1985.

7. H. Jonsson, O. Nived, G. Sturfelt, S. Valind, and B. Jonson. Lung function in patients with systemic lupus erythematosus and persistent chest symptoms. *Br J Rheumatol*, 28(6):492–9, 1989.

8. P. Wollmer, L. Eriksson, B. Jonson, K. Jakobsson, M. Albin, S. Skerfving, and H. Welinder. Relation between lung function, exercise capacity, and exposure to asbestos cement. *Br J Ind Med*, 44(8):542–9, 1987.

9. F. R. Bode, J. Dosman, R. R. Martin, H. Ghezzo, and P. T. Macklem. Age and sex differences in lung elasticity, and in closing capacity in nonsmokers. *J Appl Physiol*, 41(2):129–35, 1976.

10. G. J. Gibson, N. B. Pride, C. O'Cain, and R. Quagliato. Sex and age differences in pulmonary mechanics in normal nonsmoking subjects. *J Appl Physiol*, 41(1):20–5, 1976.

11. R. J. Knudson, D. F. Clark, T. C. Kennedy, and D. E. Knudson. Effect of aging alone on mechanical properties of the normal adult human lung. *J Appl Physiol*, 43(6):1054–62, 1977.

12. J. M. Turner, J. Mead, and M. E. Wohl. Elasticity of human lungs in relation to age. *J Appl Physiol*, 25(6):664–71, 1968.

13. J. C. Yernault, D. Baran, and M. Englert. Effect of growth and aging on the static mechanical lung properties. *Bull Eur Physiopathol Respir*, 13(6):777–88, 1977.

14. T. G. Babb and J. R. Rodarte. Mechanism of reduced maximal expiratory flow with aging. *J Appl Physiol*, 89(2):505–11, 2000.

15. R. Begin, Jr. Renzetti, A. D., A. H. Bigler, and S. Watanabe. Flow and age dependence of airway closure and dynamic compliance. *J Appl Physiol*, 38(2):199–207, 1975.

16. J. E. Cohn and H. D. Donoso. Mechanical properties of lung in normal men over 60 years old. *J Clin Invest*, 42:1406–10, 1963.

17. D. G. Ashbaugh, D. B. Bigelow, T. L. Petty, and B. E. Levine. Acute respiratory distress in adults. *Lancet*, 2(7511):319–23, 1967.

18. M. B. Amato, C. S. Barbas, D. M. Medeiros, R. B. Magaldi, G. P. Schettino, G. Lorenzi-Filho, R. A. Kairalla, D. Deheinzelin, C. Munoz, R. Oliveira, T. Y. Takagaki, and C. R. Carvalho. Effect of a protective-ventilation strategy on mortality in the acute respiratory distress syndrome. *N Engl J Med*, 338(6):347–54, 1998.

19. E. Roupie, M. Dambrosio, G. Servillo, H. Mentec, S. el Atrous, L. Beydon, C. Brun-Buisson, F. Lemaire, and L. Brochard. Titration of tidal volume and induced hypercapnia in acute respiratory distress syndrome. *Am J Respir Crit Care Med*, 152(1):121–8, 1995.

20. K. G. Hickling. The pressure-volume curve is greatly modified by recruitment. A mathematical model of ARDS lungs. *Am J Respir Crit Care Med*, 158(1):194–202, 1998.

21. B. Jonson and C. Svantesson. Elastic pressure-volume curves: what information do they convey? *Thorax*, 54(1):82–7, 1999.

22. P. Pelosi, M. Goldner, A. McKibben, A. Adams, G. Eccher, P. Caironi, S. Losappio, L. Gattinoni, and J. J. Marini. Recruitment and derecruitment during acute respiratory failure: an experimental study. *Am J Respir Crit Care Med*, 164(1):122–30, 2001.

23. S. Crotti, D. Mascheroni, P. Caironi, P. Pelosi, G. Ronzoni, M. Mondino, J. J. Marini, and L. Gattinoni. Recruitment and derecruitment during acute respiratory failure: a clinical study. *Am J Respir Crit Care Med*, 164(1):131–40, 2001.

24. B. Jonson, J. C. Richard, C. Straus, J. Mancebo, F. Lemaire, and L. Brochard. Pressure-volume curves and compliance in acute lung injury: evidence of recruitment above the lower inflection point. *Am J Respir Crit Care Med*, 159(4 Pt 1):1172–8, 1999.

25. E. De Robertis, G. Servillo, R. Tufano, and B. Jonson. Aspiration of dead space allows isocapnic low tidal volume ventilation in acute lung injury. Relationships to gas exchange and mechanics. *Intensive Care Med*, 27(9):1496–503, 2001.

26. S. M. Maggiore, B. Jonson, J. C. Richard, S. Jaber, F. Lemaire, and L. Brochard. Alveolar derecruitment at decremental positive end-expiratory pressure levels in acute lung injury. Comparison with the lower inflection point, oxygenation, and compliance. *Am J Respir Crit Care Med*, 164(5):795–801, 2001.

27. P. C. Rimensberger, P. N. Cox, H. Frndova, and A. C. Bryan. The open lung during small tidal volume ventilation: concepts of recruitment and "optimal" positive end-expiratory pressure. *Crit Care Med*, 27(9):1946–52, 1999.

28. P. C. Rimensberger, G. Pristine, B. M. Mullen, P. N. Cox, and A. S. Slutsky. Lung recruitment during small tidal volume ventilation allows minimal positive end-expiratory pressure without augmenting lung injury. *Crit Care Med*, 27(9):1940–5, 1999.

29. J. Ingimarsson, L. J. Björklund, A. Larsson, and O. Werner. The pressure at the lower inflexion point has no relation to airway collapse in surfactant-treated premature lambs. *Acta Anaesthesiol Scand*, 45(6):690–5, 2001.

30. F. Rohrer. Der Strömungswiderstand in den menschlichen Atemwegen und der Einfluss der unregelmässigen Verzweigung des Bronchialsystems auf den Atmungsverlauf in verschiedenen Lungenbezirken. *Archiv für die gesamte Physiologie*, 162:225–299, 1915.

31. C. Allander, S. Ingelstedt, B. Jonson, and H. Westling. Constant volume flow. An aid in respiratory investigation. *Med Exp Int J Exp Med*, 11:253–8, 1964.

32. B. Jonson. A method for determination of pulmonary elastic recoil and resistance at a regulated flow rate. *Scand J Clin Lab Invest*, 24(2):115–25, 1969.

33. D. Matamis, F. Lemaire, A. Harf, C. Brun-Buisson, J. C. Ansquer, and G. Atlan. Total respiratory pressure-volume curves in the adult respiratory distress syndrome. *Chest*, 86(1):58–66, 1984.

34. P. Levy, T. Similowski, C. Corbeil, M. Albala, R. Pariente, J. Milic-Emili, and B. Jonson. A method for studying the static volume-pressure curves of the respiratory system during mechanical ventilation. *J Crit Care*, 4(2):83–89, 1989.

35. L. Gattinoni, D. Mascheroni, E. Basilico, G. Foti, A. Pesenti, and L. Avalli. Volume/pressure curve of total respiratory system in paralysed patients: artefacts and correction factors. *Intensive Care Med*, 13(1):19–25, 1987.

36. J. Dall'ava-Santucci, A. Armaganidis, F. Brunet, J. F. Dhainaut, G. L. Chelucci, J. F. Monsallier, and A. Lockhart. Causes of error of respiratory pressure-volume curves in paralyzed subjects. *J Appl Physiol*, 64(1):42–9, 1988.

37. P. M. Suratt and D. Owens. A pulse method of measuring respiratory system compliance in ventilated patients. *Chest*, 80(1):34–8, 1981.

38. G. Servillo, C. Svantesson, L. Beydon, E. Roupie, L. Brochard, F. Lemaire, and B. Jonson. Pressure-volume curves in acute respiratory failure: automated low flow inflation versus occlusion. *Am J Respir Crit Care Med*, 155(5):1629–36, 1997.

39. C. Svantesson, B. Drefeldt, S. Sigurdsson, A. Larsson, L. Brochard, and B. Jonson. A single computer-controlled mechanical insufflation allows determination of the pressure-volume relationship of the respiratory system. *J Clin Monit Comput*, 15(1):9–16, 1999.

40. T. Similowski, P. Levy, C. Corbeil, M. Albala, R. Pariente, J. P. Derenne, J. H. Bates, B. Jonson, and J. Milic-Emili. Viscoelastic behavior of lung and chest wall in dogs determined by flow interruption. *J Appl Physiol*, 67(6):2219–29, 1989.

41. J. H. Bates, M. S. Ludwig, P. D. Sly, K. Brown, J. G. Martin, and J. J. Fredberg. Interrupter resistance elucidated by alveolar pressure measurement in open-chest normal dogs. *J Appl Physiol*, 65(1):408–14, 1988.

42. C. Svantesson, J. John, V. Taskar, E. Evander, and B. Jonson. Respiratory mechanics in rabbits ventilated with different tidal volumes. *Respir Physiol*, 106(3):307–16, 1996.

43. V. M. Ranieri, R. Giuliani, T. Fiore, M. Dambrosio, and J. Milic-Emili. Volume-pressure curve of the respiratory system predicts effects of PEEP in ARDS: "occlusion" versus "constant flow" technique. *Am J Respir Crit Care Med*, 149(1):19–27, 1994.

44. J. Mead, J.L. Whittenberger, and E.P. Radford, Jr. Surface tension as a factor in pulmonary volume-pressure hysteresis. *J Appl Physiol*, 10(2):191–196, 1957.

45. B. Jonson, L. Beydon, K. Brauer, C. Månsson, S. Valind, and H. Grytzell. Mechanics of respiratory system in healthy anesthetized humans with emphasis on viscoelastic properties. *J Appl Physiol*, 75(1):132–40, 1993.

46. E. Salazar and J. H. Knowles. An analysis of pressure-volume characteristics of the lungs. *J Appl Physiol*, 19:97–104, 1964.

47. J. M. Bogaard, S. E. Overbeek, A. F. Verbraak, C. Vons, H. T. Folgering, T. W. van der Mark, C. M. Roos, and P. J. Sterk. Pressure-volume analysis of the lung with an exponential and linear-exponential model in asthma and COPD. Dutch CNSLD study group. *Eur Respir J*, 8(9):1525–31, 1995.

48. J. G. Venegas, R. S. Harris, and B. A. Simon. A comprehensive equation for the pulmonary pressure-volume curve. *J Appl Physiol*, 84(1):389–95, 1998.

49. D. L. Fry. A preliminary lung model for simulating the aerodynamics of the bronchial tree. *Comput Biomed Res*, 2(2):111–34, 1968.

50. C. Svantesson, S. Sigurdsson, A. Larsson, and B. Jonson. Effects of recruitment of collapsed lung units on the elastic pressure-volume relationship in anaesthetised healthy adults. *Acta Anaesthesiol Scand*, 42(10):1149–56, 1998.

51. B. Jonson. Elastic pressure-volume curves in acute lung injury and acute respiratory distress syndrome. *Intensive Care Med*, 31(2):205–12, 2005.

52. W. A. Briscoe and A. B. Dubois. The relationship between airway resistance, airway conductance and lung volume in subjects of different age and body size. *J Clin Invest*, 37(9):1279–85, 1958.

53. B. E. Skoogh. Normal airways conductance at different lung volumes. *Scand J Clin Lab Invest*, 31(4):429–41, 1973.

54. H. H. Webb and D. F. Tierney. Experimental pulmonary edema due to intermittent positive pressure ventilation with high inflation pressures. Protection by positive end-expiratory pressure. *Am Rev Respir Dis*, 110(5):556–65, 1974.

55. J. John, V. Taskar, E. Evander, P. Wollmer, and B. Jonson. Additive nature of distension and surfactant perturbation on alveolocapillary permeability. *Eur Respir J*, 10(1):192–9, 1997.

56. V. Taskar, J. John, E. Evander, B. Robertson, and B. Jonson. Surfactant dysfunction makes lungs vulnerable to repetitive collapse and reexpansion. *Am J Respir Crit Care Med*, 155(1):313–20, 1997.

57. C. Svantesson, B. Drefeldt, and B. Jonson. The static pressure-volume relationship of the respiratory system determined with a computer-controlled ventilator. *Clin Physiol*, 17(4):419–430, 1997.

58. J. John, B. Drefeldt, V. Taskar, C. Månsson, and B. Jonson. Dynamic properties of body plethysmographs and effects on physiological parameters. *J Appl Physiol*, 77(1):152–9, 1994.

59. J. Milic-Emili, J. Mead, J. M. Turner, and E. M. Glauser. Improved technique for estimating pleural pressure from esophageal balloons. *J Appl Physiol*, 19:207–11, 1964.

60. D. P. Bolton. Static compliance measurements in the adult human lung. *J Physiol*, 207(1):28P–29P, 1970.

61. B. G. Murphy and L. A. Engel. Models of the pressure-volume relationship of the human lung. *Respir Physiol*, 32(2):183–94, 1978.

62. A. Bouhuys and B. Jonson. Alveolar pressure, airflow rate, and lung inflation in man. *J Appl Physiol*, 22(6):1086–100, 1967.

63. J. M. Bland and D. G. Altman. Statistical methods for assessing agreement between two methods of clinical measurement. *Lancet*, 1(8476):307–10, 1986.

64. J. M. Liu, E. De Robertis, S. Blomquist, P. L. Dahm, C. Svantesson, and B. Jonson. Elastic pressure-volume curves of the respiratory system reveal a high tendency to lung collapse in young pigs. *Intensive Care Med*, 25(10):1140–6, 1999.

65. E. De Robertis, J. M. Liu, S. Blomquist, P. L. Dahm, J. Thörne, and B. Jonson. Elastic properties of the lung and the chest wall in young and adult healthy pigs. *Eur Respir J*, 17(4):703–11, 2001.

66. L. Beydon, C. Svantesson, K. Brauer, F. Lemaire, and B. Jonson. Respiratory mechanics in patients ventilated for critical lung disease. *Eur Respir J*, 9(2):262–73, 1996.

67. D. G. Frazer, K. C. Weber, and G. N. Franz. Evidence of sequential opening and closing of lung units during inflation-deflation of excised rat lungs. *Respir Physiol*, 61(3):277–88, 1985.

68. H. U. Rothen, B. Sporre, G. Engberg, G. Wegenius, and G. Hedenstierna. Re-expansion of atelectasis during general anaesthesia: a computed tomography study. *Br J Anaesth*, 71(6):788–95, 1993.

69. S. Sigurdsson, C. Svantesson, A. Larsson, and B. Jonson. Elastic pressure-volume curves indicate derecruitment after a single deep expiration in anaesthetised and muscle-relaxed healthy man. *Acta Anaesthesiol Scand*, 44(8):980–4, 2000.

70. J. C. Yernault, A. De Troyer, and D. Rodenstein. Sex and age differences in intrathoracic airways mechanics in normal man. *J Appl Physiol*, 46(3):556–64, 1979.

71. M. R. Lang, G. W. Fiaux, M. Gillooly, J. A. Stewart, D. J. Hulmes, and D. Lamb. Collagen content of alveolar wall tissue in emphysematous and non-emphysematous lungs. *Thorax*, 49(4):319–26, 1994.

72. A. F. Gelb and N. Zamel. Effect of aging on lung mechanics in healthy nonsmokers. *Chest*, 68(4):538–41, 1975.

73. P. D. Wagner, R. B. Laravuso, R. R. Uhl, and J. B. West. Continuous distributions of ventilation-perfusion ratios in normal subjects breathing air and 100 per cent O2. *J Clin Invest*, 54(1):54–68, 1974.

Acknowledgements

I would like to express my sincere gratitude to all co-workers at the department of Clinical Physiology in Lund who in one way or another have contributed to this thesis.

I also want to give special thanks to:
Björn Jonson, my supervisor, for sharing your enormous knowledge and never-ending enthusiasm, for guidance, inspiration and support in many different ways.
Lisbet Niklason for help with programming and data analysis, for intelligent remarks and for always being at hand.
Ingegerd Göransson for priceless assistance and help, especially with respect to the time-consuming data collection.
Elisabeth Åström and **Berit Olsson** for assistance during animal experiments.
Kerstin Brauer for invaluable help with graphics.
Leif Uttman for discussions and collaboration.
Björn Drefeldt for programming.
Gerth-Inge Jönsson for constructing mechanical devices.
Leif Johansson and **Jens Enoksson** for thorough histopathological examinations.
Märta Granbohm for secretarial assistance.
Olle Pahlm and **Ulla Jonson** for linguistic advice.
Erik Hedström and **Einar Heiberg** for help with LaTeX.
Maj-Britt and **Allan Walter**, my parents-in-law, for help with Elsa.
Per-Olof Bitzén, my dad, for support and encouragement.
Finally, **Patrik** and our daughter **Elsa** for love, support and for patience in times when me thoughts were focused on work.

Financial support

The work was supported by grants from the Swedish Research Council (02872), the Swedish Heart Lung Foundation and Region Skåne.